

Exchange Bias and Memory Effect in Double Perovskite Sr₂FeCoO₆Pradheesh R.*,¹ Harikrishnan S. Nair*,² V. Sankaranarayanan,¹ and K. Sethupathi¹

¹*Low Temperature Physics Laboratory, Department of Physics,
Indian Institute of Technology Madras, Chennai 600036,
India.*

²*Jülich Center for Neutron Sciences-2/Peter Grünberg Institute-4,
Forschungszentrum Jülich, 52425 Jülich, Germany*

(Dated: 3 September 2021)

We report on the observation of exchange bias and *memory effect* in double perovskite Sr₂FeCoO₆. Antiphase boundaries between the ferromagnetic and antiferromagnetic regions in the disordered glassy phase is assumed as responsible for the observed effect which reflects in the cooling field dependence and temperature evolution of exchange bias field and in *training effect*. The spin glass phase itself is characterized through *memory*, *ageing* and magnetic relaxation experiments. The spin glass transition temperature, T_g , versus $H_{dc}^{2/3}$ follows the Almeida-Thouless line yielding a freezing temperature, $T_f = 73$ K. Time-dependent magnetic relaxation studies reveal the magnetization dynamics of the underlying glassy phase in this double perovskite.

PACS numbers: 75.50.Lk, 75.47.Lx, 75.50.-y

Materials that show vertical/horizontal displacement of magnetic hysteresis loop – known as exchange bias materials – are potential candidates for technological applications as spin valves¹, permanent magnets² and in magnetic recording^{3,4}. Exchange bias is observed mainly in ferromagnetic (FM)/ antiferromagnetic (AFM) bilayers⁵ but, also in nanoparticles⁶, inhomogeneous magnets,² and strongly correlated oxides like manganites,⁷ cobaltites,⁸ and in intermetallics⁹. In classical exchange bias (EB) systems, the hysteresis loop is shifted to the left of the origin and conventionally EB is defined negative. Positive EB has also been reported, for example, in metallic bilayers¹⁰ and in spin glasses¹¹. In a detailed study to distinguish between reentrant spin glass (RSG) and cluster glass (CG), exchange bias with a shift in both magnetization and field axis was observed in $\text{L}_{0.5}\text{Sr}_{0.5}\text{CoO}_3$ ¹². In this Letter, we report the observation of exchange bias in a spin glass double perovskite thereby, extending the generality of this phenomenon.

The spin glass (SG) nature of $\text{Sr}_2\text{FeCoO}_6$, with transition temperature $T_g \approx 75$ K, studied through macroscopic magnetization and structural studies using neutrons has been reported elsewhere¹³. In this paper we focus on detailed magnetization measurements in field-cooled and zero field-cooled conditions along with magnetic relaxation measurements conducted using commercial SQUID magnetometer and physical property measurement system (both M/s Quantum Design Inc.).

As the first set of magnetization measurements, field-cooled hysteresis curves at different temperatures were measured on $\text{Sr}_2\text{FeCoO}_6$. To this effect, the sample was field-cooled from 120 K to a temperature below T_g with an applied field of 50 Oe (after each $M(H)$ curve the sample was demagnetized by warming up to 120 K). The field-cooled magnetic hysteresis loops at different temperatures in the range 30 – 70 K, that show clear shifts resembling EB are presented in Fig 1 (a). The loop-shifts in the $M(H)$ plots, as seen in the figure, can signify exchange bias due to the spins at of FM/AFM, FM/SG interfaces. In $\text{Sr}_2\text{FeCoO}_6$, antisite disorder leads to SG phase at low temperature which then forms FM/SG interfaces which can cause exchange anisotropy. In order to avoid minor loop effect in the observation of a genuine EB-shift, the optimal maximum applied field (H_{max}) should be greater than the anisotropy field (H_A) of the system. From the analysis of initial magnetization at 50 K using $M = M_s(1 - a/H - b/H^2) + \chi H$ and using the relations $b = 4K_1^2/15M_s^2$ and $H_A = 2K_1/M_s$ ^{14,15}, a rough estimate of the anisotropy field $H_A = 448$ Oe was obtained (M_s is saturation magnetization, a , b are free-parameters, K_1 is anisotropy constant, χ is the high-

field susceptibility). Consequently, our hysteresis measurements were performed such that the maximum applied field $H_{max} > H_A$. Fig. 1 (b), shows that the effect of applied fields greater than 10 kOe is to diminish the effect of exchange bias. Similar effect of vanishing EB at high fields has been reported for cluster glass perovskite cobaltites¹⁶. In order to confirm that the exchange bias effect is intrinsic, we performed *training effect* experiment where the $M(H)$ curve at 50 K is recorded in field-cooled condition for 12 continuous loops. In Fig 1 (c), a magnified view of the 1st and 12th loops are presented showing a clear shift which is typical of the response from exchange biased systems and hints at the metastable nature of the interface¹⁷. Field-cooled hysteresis curves at 50 K were measured as a function of different cooling fields, H_{FC} . The exchange bias field was estimated from the $M(H)$ loops as, $|H_{EB}| = |(H_+ + H_-)/2|$; H_+ and H_- are the positive and negative intercepts of the magnetization curve with the field axis. The variation of H_{EB} as a function of H_{FC} and temperature are shown in Fig. 2 (a) and (b) respectively. In order to probe RSG features in the present system, we performed field-cooled hysteresis measurements at different cooling fields as suggested in Mukherjee et. al.¹². The resulting $M(H)$ plots are presented in Fig 2 (c). Displaced hysteresis loops are evident which, with increasing H_{FC} intersect the H -axis at a progressively higher negative values. Similar feature has been observed in $\text{La}_{0.5}\text{Sr}_{0.5}\text{CoO}_3$ ¹² and signifies the presence of FM clusters.

In the case of spin glass systems, the peak at T_g in the imaginary part of ac magnetic susceptibility shifts to low temperature with increasing value of superimposed dc field. The evolution of T_g with applied magnetic field can be explained by Almeida-Thouless (*AT*) line in a H - T phase diagram¹⁸. The *AT* line is described by the equation,

$$\frac{H_{dc}(T)}{\Delta J} = (1 - T_g/T_C)^\alpha \quad (1)$$

Here ΔJ is the width of the distribution of exchange interactions, H_{dc} is the superimposed dc magnetic field and T_C is the transition temperature. Fig 3 (a) is the plot of T_g versus $H_{dc}^{2/3}$ for $\text{Sr}_2\text{FeCoO}_6$ which shows a decrease in T_g with applied field. A fit to the variation of T_g with field assuming the critical exponent $\alpha = 3/2$ gives straight line fit satisfying the *AT* equation and confirms the spin glass nature of $\text{Sr}_2\text{FeCoO}_6$. Linear behaviour with the critical exponent being 3/2 is observed for low fields ($\mu_0 H < 1$ T). Extrapolating the fit to both the axes, we obtain the freezing temperature (T_f) and the critical field (H_{cr}) as 73 K and 116 Oe respectively. The conformity with *AT*-line has been observed in intrinsically ex-

change biased $Zn_xMn_{3-x}O_4$ solid solutions¹⁹. For reentrant spin glass systems, the disorder extends to the whole volume resulting in the shift of T_f to lower temperatures with increase in magnetic field²⁰.

In order to further test the glassy magnetic ground state in Sr_2FeCoO_6 , *memory* experiments were conducted, for which, the sample is first zero field-cooled to low temperatures at a constant cooling rate, while recording magnetization. While cooling, intermediate stops are administered below T_c when the measurement is stopped (for 2 h) and magnetization is allowed to relax. After reaching the lowest possible temperature, the sample is heated back at a constant heating rate without administering any stops and magnetization is recorded. For comparison, a reference curve where no stops are administered is also recorded. The cooling, heating, reference and the derivative of the heating curve, dM/dT , are presented in Fig 3 (b). Clear ‘*dips*’ in magnetization of the cooling curve are discernible where the measurement was stopped. The signatures of *memory* effect is clear in the heating cycle where the steps are recovered at the same temperature points. This is clearly visible in the plot of dM/dT . Observation of *memory* effect is a confirmation of the magnetic glassy state and has been reported in canonical spin glasses and phase separated manganites that show spin glass-like ground states.

In order to study the magnetic relaxation mechanisms stemming from the underlying magnetic glassy state, time dependent magnetization with different wait times were recorded at 50 K. For these measurements, the sample was zero field-cooled to 50 K, a wait time t_w was administered and then the magnetization was measured as a function of time. Evident from Fig 4 (a), a clear dependence on t_w can be seen wherein the system becomes magnetically stiffer as the wait time increases; which is common among canonical spin glasses. Fig 4 (b) shows time-dependent magnetization at $t_w = 3600$ s but at different temperatures. The time-dependent magnetization was fitted well with a stretched exponential of the form

$$M(t) = M_0 - M_g \exp[-(\frac{t}{t_r})^{1-n}] \quad (2)$$

where M_0 is the intrinsic ferromagnetic moment, M_g is the glassy component of the moment, t_r is the characteristic time component and n is the stretched exponential exponent. Eqn. (2) is similar to Kohlrausch law²¹ which is used to explain magnetic, dielectric and optical phenomena where relaxation mechanisms play a important role in the dynamics. The exponent in Eqn. (2) is temperature dependent, and according to the percolation model, varies in

the range $\frac{1}{3} \leq n \leq 1^{22}$. Table I shows the parameters obtained from the fit according to Eqn (2). The values of n and M_0 are independent of t_w while the characteristic time scale t_r varies with t_w typical of canonical spin glasses²³. The characteristic time varies slowly with the wait time, but the dependence of t_r on t_w implies that it is in a non-equilibrium state and that of the *memory effect*. Negative temperature cycling of magnetization in zero field-cooled (ZFC) and field-cooled (FC) protocols were also performed to complement the *memory effect*. In the ZFC protocol, the sample was cooled down to 35 K in ZFC mode and a field of 100 Oe was applied to measure magnetization for time t_1 . Further, the sample was cooled down to 30 K, the field is switched off, immediately after which the magnetization is recorded for another time t_2 . After t_2 the system is taken back to 35 K and magnetization measured for time t_3 . In the above measurement, $t_1 = t_2 = t_3 = 3600$ s. Fig 4 (c) shows the ZFC temperature cycling where the effect of *memory* is observable even after *aging* at lower temperature. Fig 4 (d) illustrates the same experiment as in (c) but, in FC protocol. Similar measurements (ZFC and FC) but in heating cycle were performed the results of which are given in Fig 4 (e) and (f). An asymmetric response is observed which means that there is no *memory* while heating the sample.

The relaxation measurements confirms the spin glass nature of $\text{Sr}_2\text{FeCoO}_6$ and can be concluded that the observed exchange bias is seen in the spin glass phase. Exchange bias systems with FM/SG interfaces are known to show exponential decrease in H_{EB} with temperature⁷. In such a scenario, the SG phase forms the frozen phase where magnetization is irreversible while that of the FM phase is reversible. In the present case, we assume a minority FM phase which coexist in a majority AFM disordered (glassy) phase as deduced from the hysteresis curves and lack of saturation magnetization. With reduction in temperature, increasing number of disordered AFM (or glassy) domains freeze and this progressive freezing leads to enhancement of H_{EB} at low temperature. The dependence of H_{EB} on H_{FC} is understood based on the competition between the Zeeman coupling energy and the exchange energies at the interfaces. At low cooling fields, field-cooling induces progressive enhancement of freezing of domains and hence H_{EB} increases whereas at high cooling fields, Zeeman energy overcomes the magnetic interactions at the interface.

In conclusion, we report the observation of exchange bias in the double perovskite $\text{Sr}_2\text{FeCoO}_6$ which is a spin glass. The claim of intrinsic exchange bias is supported through field-cooled hysteresis measurements, dependence of exchange bias fields on cooling fields and tempera-

ture, *training effect* etc. Interface magnetic interactions between FM regions and SG domains are believed to be the origin of observed exchange bias. The underlying spin glass phase is further characterized through the conformation with *AT*-line, *memory* and *aging* effects and magnetic relaxation.

The authors acknowledge the Department of Science and Technology (DST), India for the financial support for providing the facilities used in this study (Grant No. SR/FST/PSII-002/2007) and (Grant No. SR/NM/NAT-02/2005).

* Authors contributed equally to this work.

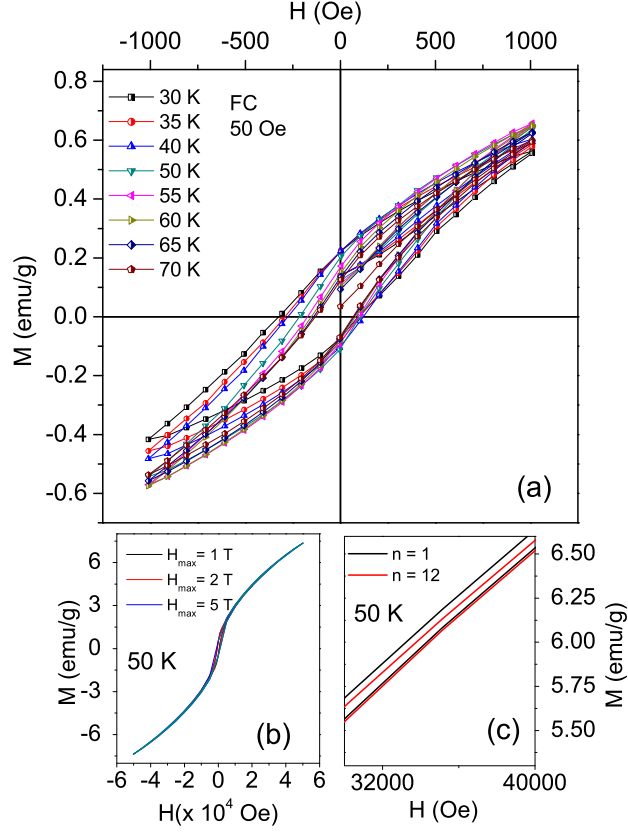


FIG. 1. (colour online) (a) Field-cooled (50 Oe) isothermal magnetization of $\text{Sr}_2\text{FeCoO}_6$ at different temperatures below T_g . The field range is limited to ± 1000 Oe (H_{max}) which is greater than H_A (i.e., $H_{max} > H_A$). (b) Hysteresis plots at different H_{max} where exchange bias disappears. (c) *Training effect* at 50 K observed with 12 loops.

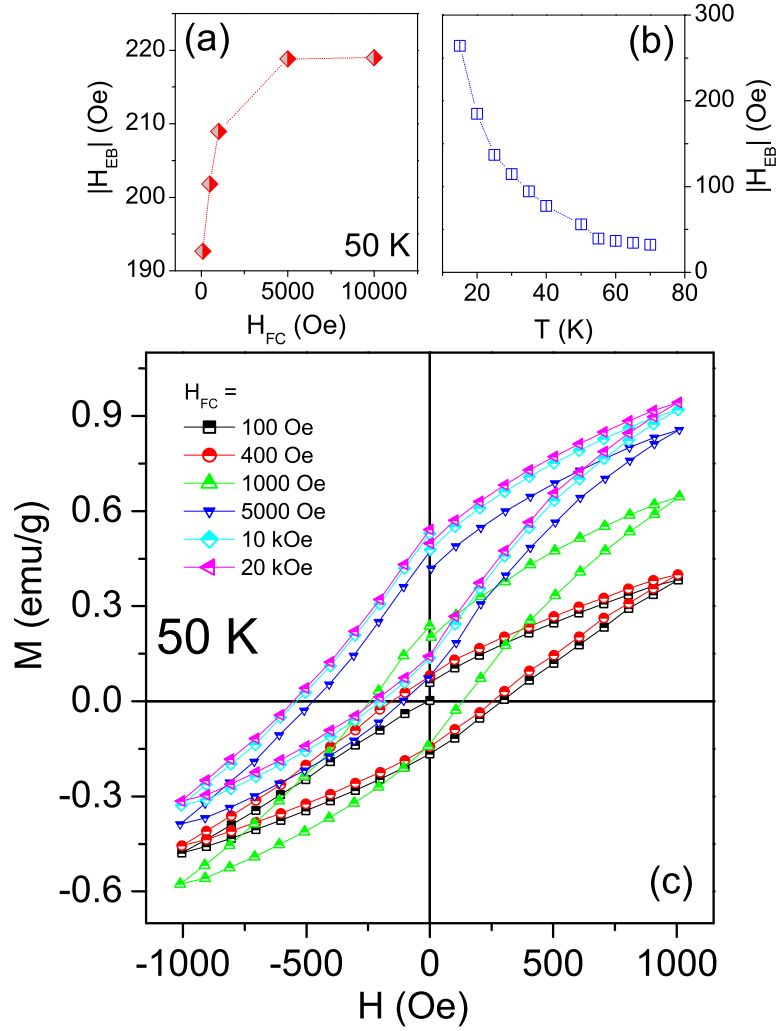


FIG. 2. (colour online) Exchange bias field H_{EB} plotted against (a) H_{FC} and (b) temperature conform to typical exchange bias characteristics. (c) The field-cooled hysteresis curves at different cooling fields up to 20 kOe display vertical displacement that signify FM clusters present in the system.

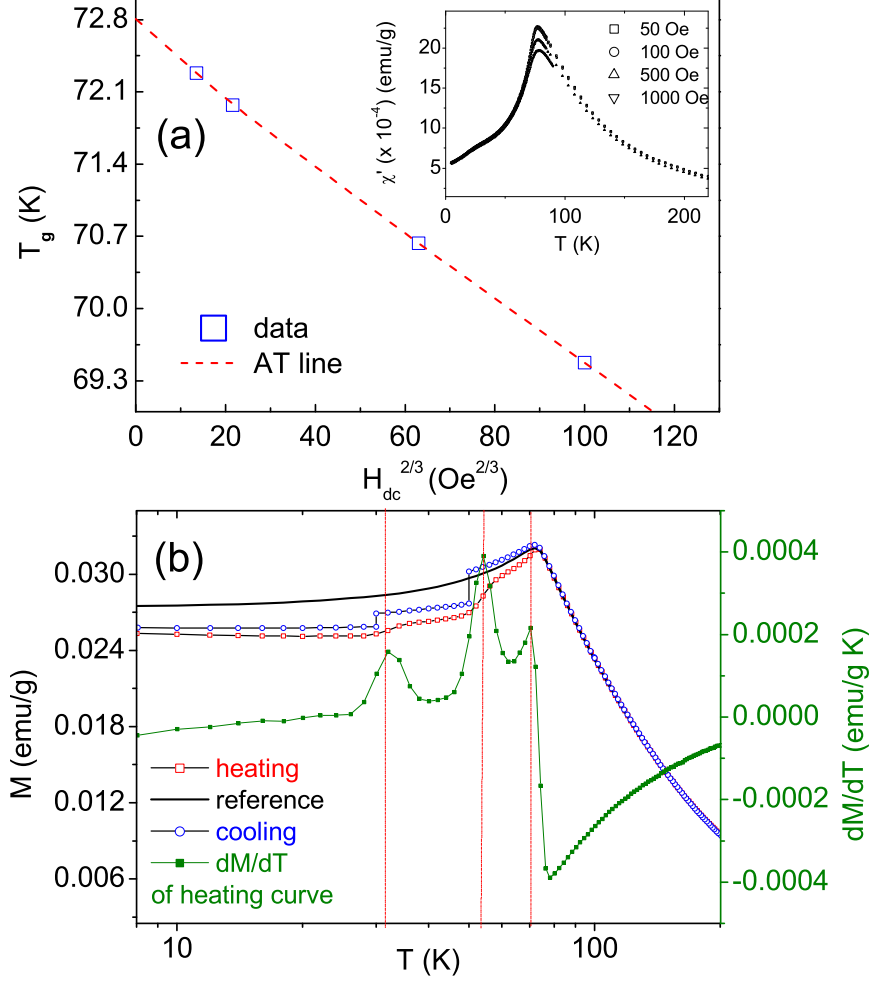


FIG. 3. (colour online) (a) T_g vs $H_{dc}^{2/3}$ plot for $\text{Sr}_2\text{FeCoO}_6$ where H_{dc} is the superimposed dc field and the dashed-line shows the fit according to Eqn. 1. The inset shows the real part of ac susceptibility, $\chi'(T)$, at different applied dc fields. (b) *Memory* effect in $\text{Sr}_2\text{FeCoO}_6$. The stops administered during the cooling curve, where the measurement is halted, are recovered in the heating cycle. The derivative plots clearly show the recovered stops. For comparison, a reference measurement curve (without stops) is also presented.

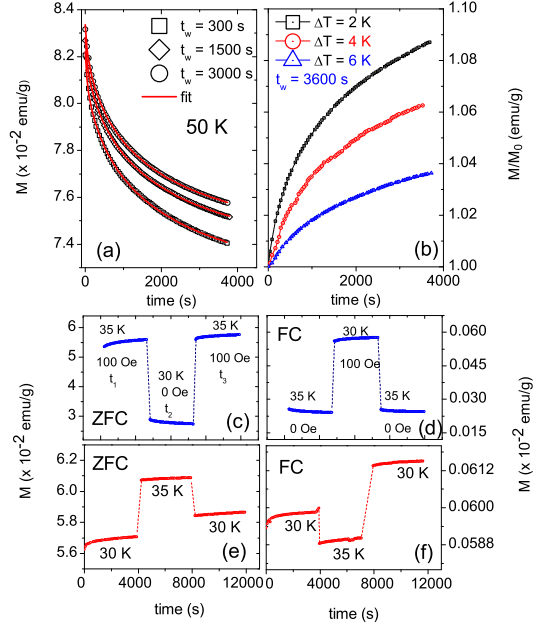


FIG. 4. (colour online) (a) Time-dependent magnetization of $\text{Sr}_2\text{FeCoO}_6$ at 50 K for three different wait times. The solid lines are fit to the eqn (2). (b) The time-dependent magnetization with a wait time of $t_w = 3600$ s. Signatures of *aging* are present in relaxation experiments in both ZFC ((c), (e)) and FC ((d), (f)) protocols. (c) and (d) show negative temperature cycling in ZFC and FC mode respectively while (e) and (f) show the same plots in warming mode. Asymmetric response is clearly seen for the warming mode.

TABLE I. The parameters, M_0 , M_g , t_r and n obtained by fitting the time-dependent magnetization at different wait times using eqn 2.

t_w (s)	M_0 (emu/g)	M_g (emu/g)	t_r (s)	n
300	0.009(3)	0.074(1)	1590(1)	0.43(1)
1500	0.009(2)	0.073(2)	1671(2)	0.41(2)
3000	0.0102(3)	0.071(2)	1705(1)	0.41(5)

REFERENCES

- ¹B. G. Park, J. Wunderlich, X. Martí, V. Holý, Y. Kurosaki, M. Yamada, H. Yamamoto, A. Nishide, J. Hayakawa, H. Takahashi et al., *Nature Mater.*, **10**(5), 347 (2011).
- ²J. Nogués and I. K. Schuller. *J. Magn. Magn. Mater*, **192**, 203 (1999).
- ³J. -W. Liao, R. K. Dumas, H. -C. Hou, Y. -C. Huang, W. -C. Tsai, L. -W. Wang, D. -S. Wang, M. -S. Lin, Y. -C. Wu, R. -Z. Chen, et al., *Phys. Rev. B*, **82**(1), 014423 (2010).
- ⁴I. V. Roshchin, O. Petravic, R. Morales, Z. P. Li, X. Batlle, I. K. Schuller. US Patent 7,764,454 (2010).
- ⁵M. D. Stiles and R. D. McMichael. *Phys. Rev. B*, **63**, 064405 (2001).
- ⁶V. Skumryev, S. Stoyanov, Y. Zhang, G. Hadjipanayis, D. Givord, and J. Nogués. *Nature*, **423**(6942), 850 (2003).
- ⁷S. Karmakar, S. Taran, E. Bose, B. K. Chaudhuri, C. P. Sun, C. L. Huang, and H. D. Yang. *Phys. Rev. B*, **77**, 144409, (2008).
- ⁸Y. -k Tang, Y. Sun, and Z. -h Cheng. *Phys. Rev. B*, **73**, 174419, (2006).
- ⁹X. H. Chen, K. Q. Wang, P. H. Hor, Y. Y. Xue, and C. W. Chu. *Phys. Rev. B*, **72**, 054436, (2005).
- ¹⁰J. Nogués, D. Lederman, T. J. Moran, and I. K. Schuller. *Phys. Rev. Lett.*, **76**, 4624 (1996).
- ¹¹M. Ali, P. Adie, C. H. Marrows, D. Greig, B. J. Hickey, and R. L. Stamps. *Nature Mater.*, **6**, 70 (2007).
- ¹²S. Mukherjee, R. Ranganathan, P. S. Anilkumar, and P. A. Joy. *Phys. Rev. B*, **54**(13), 9267 (1996).
- ¹³R. Pradheesh, Harikrishnan S. Nair, C. M. N. Kumar, Jagat Lamsal, R. Nirmala, P. N. Santhosh, W. B. Yelon, S. K. Malik, V. Sankaranarayanan, and K. Sethupathi. *J. Appl. Phys.*, **111**(5), 053905 (2012).
- ¹⁴S. V. Andreev, M. I. Bartashevich, V. I. Pushkarsky, V. N. Maltsev, L. A. Pamyatnykh, E. N. Tarasov, N. V. Kudrevatykh, and T. Goto. *J. Alloys and Comp.*, **260**(1), 196–200 (1997).
- ¹⁵M. Patra, M. Thakur, K. De, S. Majumdar, and S. Giri. *J. Phys.: Condens. Matter*, **21**, 078002 (2009).
- ¹⁶W. Luo and F. Wang. *Appl. Phys. Lett.*, **90**, 162515 (2007).

- ¹⁷S. Giri, M. Patra, and S. Majumdar. *J. Phys.: Condens. Matter*, **23**, 073201 (2011).
- ¹⁸J. R. L. de Almeida and R. Bruinsma. *Phys. Rev. B*, **35**, 7267 (1987).
- ¹⁹D. P. Shoemaker, E. E. Rodriguez, R. Seshadri, I. S. Abumohor, and T. Proffen. *Phys. Rev. B*, **80**, 144422 (2009).
- ²⁰B. Martinez, X. Obradors, Ll. Balcells, A. Rouanet, and C. Monty. *Phys. Rev. Lett.*, **80**(1), 181 (1998).
- ²¹R. G. Palmer, D. L. Stein, E. Abrahams, and P. W. Anderson. *Phys. Rev. Lett.*, **53**(10), 958 (1984).
- ²²R. Böhmer, K. L. Ngai, C. A. Angell, and D. J. Plazek. *J. Chem. Phys.*, **99**(5), 4201 (1993).
- ²³R. V. Chamberlin. *Phys. Rev. B*, **30**(9), 5393 (1984).